ChemPubSoc Europe

DOI: 10.1002/ejic.201700439

EurJIC European Journal of Inorganic Chemistry

Full Paper

Photosubstitution in Ru Complexes

Photosubstitution of Monodentate Ligands from Ru^{II}–Dicarboxybipyridine Complexes

Rolando M. Caraballo,[a,b] Pablo Rosi,[a] José H. Hodak,[a,b] and Luis M. Baraldo*[a,b]

Abstract: We report the photophysical and photochemical properties of Ru^{II}–polypyridine complexes $[Ru(bpy)(dcbpy)py_2]^{2+}$ $(\mathbf{1})^{2+}$ and $[Ru(dcbpy)_2py_2]^{2+}$ $(\mathbf{2})^{2+}$ (bpy = 2,2′-bipyridine, dcbpy = 4,4′-dicarboxy-2,2′-bipyridine, py = pyridine). These complexes combine a monodentate ligand with a chelate bipyridine substituted with carboxylate groups. At low pH, both complexes present metal-to-ligand charge transfer absorption bands in the visible region and room-temperature photoluminescence with long excited-state lifetimes (τ > 200 ns). At physiological pH, their absorption and emission maxima are displaced to higher energies, with a significant reduction of their emission lifetime. These species show photosubstitution of the monodentate pyridine upon irradiation at 450 nm. At low pH, the quantum yield for this process is very low, but at physiological pH, they are very active, with a $\varphi_{PS,450}$ value of 0.14 for $(\mathbf{1})^{2+}$ and of 0.17 for $(\mathbf{2})^{2+}$. The products of photosubstitution were identified as monoaquo complexes. Both the reactants and the products of the photosubstitution show photoluminescence, but with very different lifetimes, making it possible to monitor the reaction by the time constant of their decay. The ability of complexes $(\mathbf{1})^{2+}$ and $(\mathbf{2})^{2+}$ to photorelease monodentate ligands at physiological pH makes them attractive candidates for the delivery of biomolecules linked to more complex structures through the carboxylate functional group.

Introduction

The unique properties of the Ru^{II}–polypyridines have prompted their use in different fields, such as photochemotherapy (PCT),[1,2] caged compounds,[3] devices,[4] and sensitizer dyes for solar-energy conversion.[5,6] Their use as caged compounds is based on the well-reported property that substitution of monodentate ligands can be triggered by the absorption of visible light.[7] The process has been attributed to the presence of a triplet ligand-field excited state (^{3}LF) that lies very close in energy to the initially populated ^{3}MLCT (metal-to-ligand charge transfer) state and can be thermally populated.[8] This provides a pathway to the deactivation of the emitting state and has a strong impact on its lifetime.

Cage compounds or phototriggers are molecules that – upon absorption of visible light – release a fragment of interest, usually a molecule of biological relevance.[9] Since the first report,[10] transition-metal complexes have been actively explored for this purpose.[11] The so-called RuBi family of compounds[12] {RuBi = $[Ru(bpy)_2LL']^n$, with L and L′ monodentate ligands} presents some advantages, compared with other systems frequently used, such as the stability of the caged molecule and the possibility of releasing the molecule using visible light or infrared light under a two-photon regime.[13] This cage has been used for the release of neurotransmitters, such as 4-aminopyridine,[13] serotonin,[14] GABA,[15] glutamate,[16] nicotine,[17] dopamine,[18] and drugs with therapeutic value.[19–21]

Inclusion of functional groups on the bpy ligands could greatly increase the applicability of these compounds, adding properties like molecular recognition and transport improvement. One of the most interesting groups to be added is carboxylate. It has been extensively used to attach the Ru^{II} chromophore to the surface of semiconductors and promote injection of the electrons into the conduction band in different schemes to make use of solar energy, such as dye-sensitized photovoltaic cells[5] or photocatalytic devices.[6,22] This linker has also been used to attach Ru^{II} complexes to proteins through free amine groups, for the detection of purification processes or as a part of energy-transfer studies.[23] Given the rich literature on the covalent incorporation of Ru^{II} complexes to surfaces and biomolecules,[24] the extension of this strategy to RuBi cages seems very possible, provided that the attachment retains its ability to photorelease the caged molecule. Besides the ability to covalently link the RuBi cage, the presence of free carboxylate groups could be used to tune other properties, like solubility, in different environments.

The modification of bpy ligands could also have an impact on the photophysical properties; hence, the exploration of suitable models is required in order to evaluate the potential of the substituted Ru^{II}–polypyridines as caging fragments. In fact, a previous report indicates that the complex $[Ru(deeb)_2py_2]^{2+}$ in acetonitrile [deeb = 4,4′-bis(ethoxycarbonyl)-2,2′-bipyridine]

[a] Universidad de Buenos Aires, Facultad de Ciencias Exactas y Naturales, Departamento de Química Inorgánica, Analítica y Química Física, Pabellón 2, Ciudad Universitaria, C1428EHA, Buenos Aires, Argentina
E-mail: baraldo@qi.fcen.uba.ar
http://www.inquimae.fcen.uba.ar/baraldo_luismario.htm
[b] CONICET – Universidad de Buenos Aires, Instituto de Química-Física de Materiales, Ambientes y Energía (INQUIMAE), Buenos Aires, Argentina

Supporting information and ORCID(s) from the author(s) for this article are available on the WWW under https://doi.org/10.1002/ejic.201700439.

shows no significant photolabilization of the py monodentate ligands.[25]

Here, we report the photophysical properties in aqueous solutions of ruthenium complexes containing at least one dcbpy ligand, together with monodentate pyridine ligands. We have chosen pyridine as our model monodentate ligand, as it is related to complex $[Ru(bpy)_2py_2]^{2+}$, which has been thoroughly studied,[26–29] and hence, a comparison with its properties is possible. Also, the py ligand, like many other amines, forms a strong bond with Ru^{II}, so it is a representative model. These complexes show very limited photorelease activity in acidic solutions, but are very active at physiological pH. The latter property makes them good candidates for the development of modified RuBi-caged compounds.

Results and Discussion

We decided to prepare complexes with varying degrees of carboxylate-group substitution at the ligands to assess the impact of the functional-group addition. We avoided the ligands with only one carboxylate group, as they will lead to isomers, with the ring substituted by the carboxylate *cis* or *trans* to one of the pyridine ligands. The separation of this type of isomers is not easy, and their presence would increase the number of signals in the NMR spectra, making it very difficult to analyze the photolysis products by this technique. So, we restricted ourselves to the incorporation of one or two dcbpy ligands.

To prepare the complex $(\mathbf{1})^{2+}$ containing only one dcbpy ligand (Scheme 1), we took advantage of the intermediate complex *cis*(Cl),*cis*(*S*)-Ru(bpy)(dmso-S)$_2$Cl$_2$, which can be prepared with a yield better than 90 %.[30] The reaction of this precursor with the 4,4′-bis(methoxycarbonyl)-2,2′-bipyridine (dmebpy) ligand in methanol affords the desired dichloride complex in good yield. Reaction of the latter in an aqueous solution of pyridine, followed by treatment with a hot basic solution, gives complex $(\mathbf{1})^{2+}$. The synthesis of $(\mathbf{2})^{2+}$ involves the reflux of the reported dichloride *cis*-$[Ru(dcbpy)_2Cl_2]$[31] in an aqueous solution of pyridine, followed by dissolution in a basic solution and the precipitation of the PF_6^- salt upon acidification.

The electronic spectra of complexes $(\mathbf{1})^{2+}$ and $(\mathbf{2})^{2+}$ in acidic (pH 1.1) and basic (pH 7.4) media are shown in Figure 1. All of the spectra show the expected features for an Ru–polypyridine. For example, the spectrum of $(\mathbf{2})^{2+}$ in an acidic medium shows sharp transitions at 242 and 311 nm, which we assign as centered on the dcbpy ligand [π*(dcbpy)←π(dcbpy)], and two wide transitions at 352 and 489 nm that correspond to CT transitions involving the dcbpy ligand and the metal atom [π*(dcbpy)←dπ(Ru)]. The latter transition appears at almost the same energy as the one for $[Ru(deeb)_2py_2]^{2+}$ (488 nm),[25] but it is redshifted compared with the one observed for the complex $[Ru(bpy)_2py_2]^{2+}$ (456 nm).[27] This is a consequence of the lower energy of the π* orbitals of the dcbpy ligand relative to those of bpy. The spectrum of $(\mathbf{1})^{2+}$ shows three maxima in the visible region instead of two, with bands at 374, 425, and 490 nm. We assign the additional band to the presence of two different acceptor ligands that result in the presence of further MLCT transitions. In basic media, the maxima of the MLCT bands of both complexes shift to higher energies (Figure 1 and Tables 1 and S1), as previously observed for other Ru–polypyridines containing the dcbpy ligand.[32–34]

Unlike the complex $[Ru(bpy)_2py_2]^{2+}$,[35] complexes $(\mathbf{1})^{2+}$ and $(\mathbf{2})^{2+}$ present strong photoluminescence (PL) at room temperature, both in acidic and basic conditions. Their excitation and emission profiles are illustrated in Figure 2. In acidic media, the emission properties for both complexes are typical for ruthenium–polypyridine complexes with emission maxima, quan-

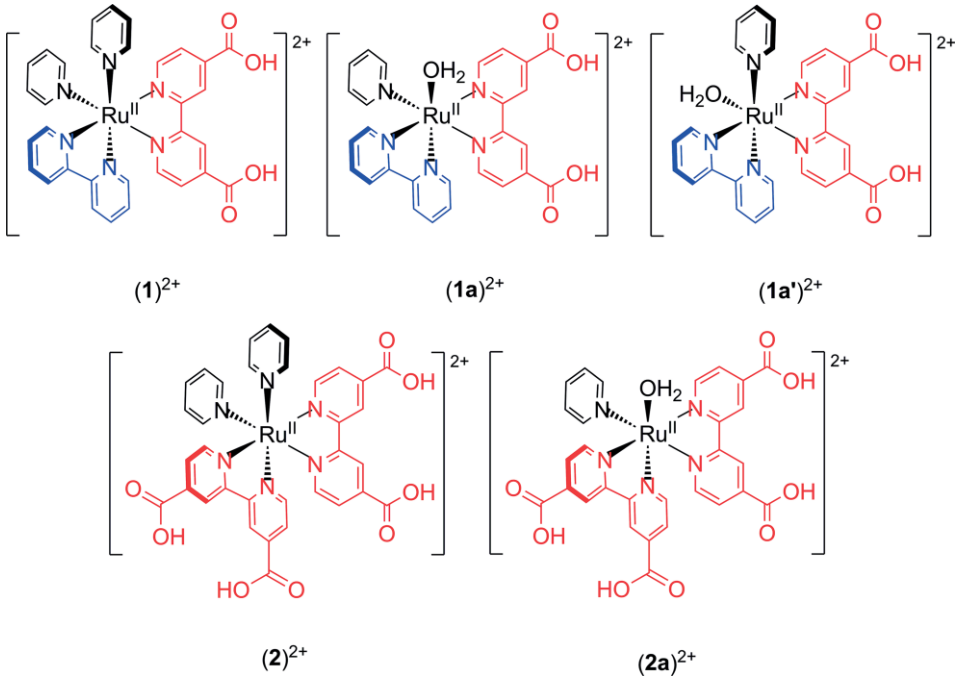

Scheme 1. Sketches of the complexes $(\mathbf{1})^{2+}$, $(\mathbf{1a})^{2+}$, $(\mathbf{1a'})^{2+}$, $(\mathbf{2})^{2+}$, and $(\mathbf{2a})^{2+}$ discussed in this work.

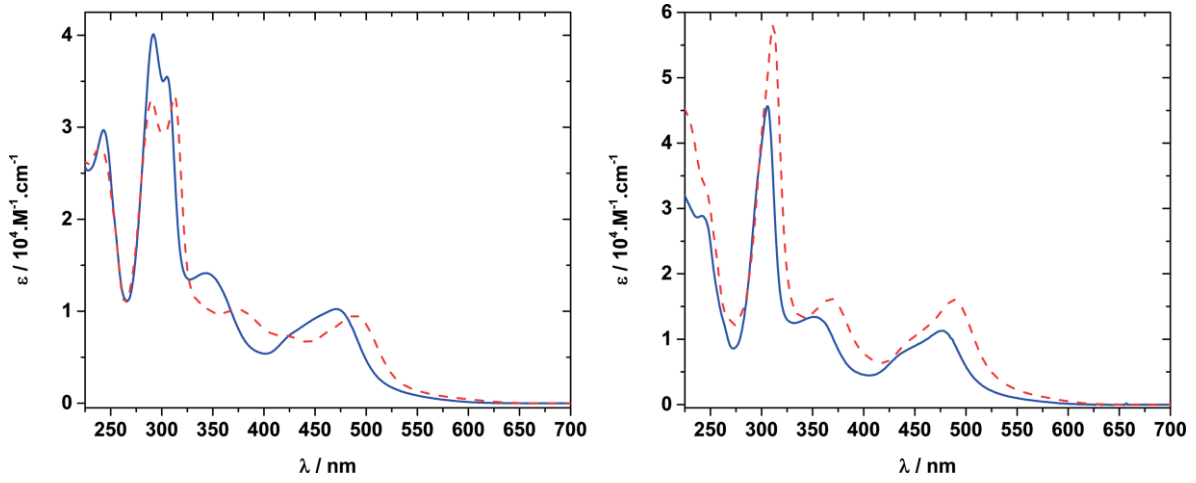

Figure 1. Electronic absorption spectra of complexes $(\mathbf{1})^{2+}$ (left) and $(\mathbf{2})^{2+}$ (right) in acidic (pH 1.1, red, dashed) and basic (pH 7.4, blue, solid) media.

Table 1. Spectroscopic properties for the deareated acetonitrile solutions of complexes $(\mathbf{1})^{2+}$, $(\mathbf{2})^{2+}$, $(\mathbf{1a})^{2+}$, and $(\mathbf{2a})^{2+}$.

Complex	pH	λ_{Abs} [nm] (ε [10^4 M^{-1} cm^{-1}])	λ_{Em} [nm] (φ_{Em} [%])	τ_{Em} [ns]
$(\mathbf{1})^{2+}$	1.1	487 (0.96)	693 (5.7)	285
	7.4	471 (1.02)	648 (0.7)	61
$(\mathbf{2})^{2+}$	1.1	489 (1.61)	668 (6.8)	378
	7.4	476 (1.13)	643 (0.6)	53
$(\mathbf{1a})^{2+}$	1.1	496 (0.97)	–	10
	7.4	484 (1.08)	626[a]	1.4
$(\mathbf{2a})^{2+}$	1.1	501 (1.67)	–	12
	7.4	489 (1.16)	650[a]	1.4
$[Ru(bpy)_2(dcbpy)]^{2+}$	1.1	482 (1.21)	695 (2.6)	260
	7.4	458 (1.53)	654 (5.5)	486
$[Ru(bpy)(dcbpy)_2]^{2+}$	1.1	481 (1.88)	668 (4.9)	417
	7.4	466 (1.64)	648 (6.6)	556

[a] The emission for these complexes is very weak, and we report the maxima of the uncorrected emission.

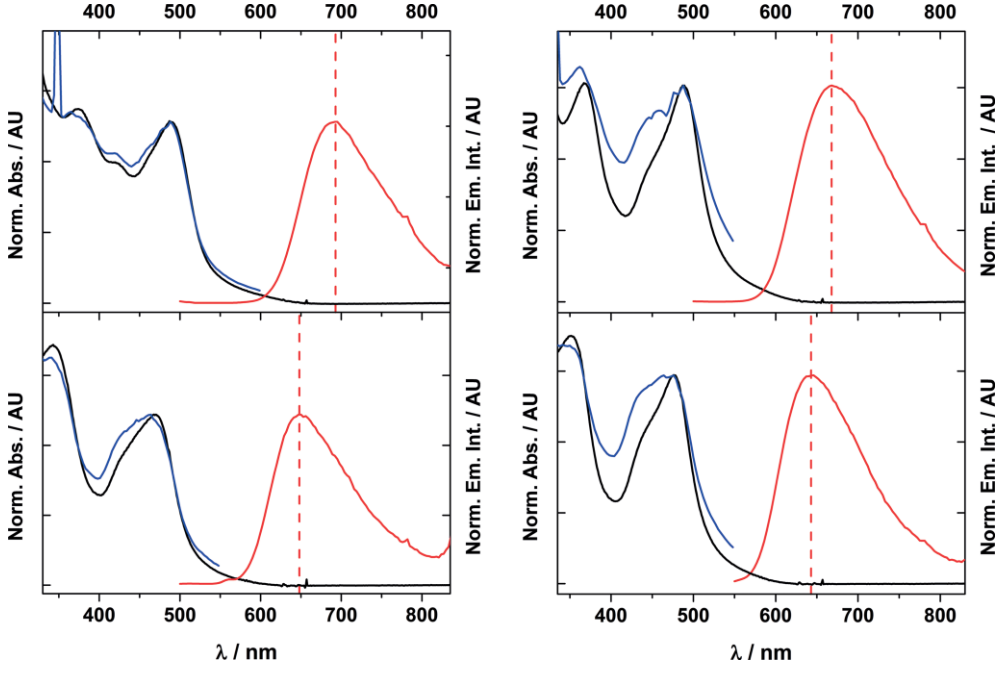

Figure 2. Absorption (black), excitation (blue), and emission spectra (red) of $(\mathbf{1})^{2+}$ (left) and $(\mathbf{2})^{2+}$ (right) in acidic (top, pH 1.1) and basic (bottom, pH 7.4) media. The emission spectra were taken with excitation at the wavelength of the maximum of the MLCT band. The excitation spectra were collected at the wavelength of the emission maximum. Absorption and excitation spectra are normalized at the wavelength of the MLCT band maximum, while emission spectra are normalized at the peak wavelength.

tum yields, and lifetimes similar to those reported for the related complexes $[Ru(bpy)_2(dcbpy)]^{2+}$ and $[Ru(bpy)(dcbpy)_2]^{2+}$ in the same medium (Table 1). The PL spectra of $(\mathbf{1})^{2+}$ are clearly centered more to the red, compared with the one of $(\mathbf{2})^{2+}$. A similar shift is observed between the emission of $[Ru(bpy)_2(dcbpy)]^{2+}$ and $[Ru(bpy)(dcbpy)_2]^{2+}$. This is due to the more basic nature of the ligands present in $(\mathbf{1})^{2+}$ and $[Ru(bpy)_2(dcbpy)]^{2+}$, which results in a stabilization of the Ru^{III} moiety present in the ^{3}MLCT states.

The PL spectra of both complexes dissolved in basic solutions are blueshifted, with an increase of energy of 1000 cm^{-1} for $(\mathbf{1})^{2+}$ and 580 cm^{-1} for $(\mathbf{2})^{2+}$. The quantum yield of the emission at pH 7.4 is greatly diminished, and an associated decrease of the emission lifetime is also observed (Table 1). At intermediate pH values, a third lifetime can be detected for both complexes, and we assign it to the mono-deprotonated species (Figures S1 and S2 and Table S2). The shorter lifetimes determined for the deprotonated species are in clear contrast with the results for $[Ru(bpy)_2(dcbpy)]^{2+}$ and other dcbpy-containing ruthenium–polypyridine complexes,[33,34] where a change to basic pH results in a blueshift of the PL spectrum, together with an increase in the intensity of the emission and a longer lifetime. The fact that the opposite trend is observed for $(\mathbf{1})^{2+}$ and $(\mathbf{2})^{2+}$ suggests that some other process could be operative in these complexes.

DFT calculations were employed to study the structure and spectra of the protonated forms of complexes $(\mathbf{1})^{2+}$ and $(\mathbf{2})^{2+}$ in water. The calculated structures for both complexes are shown in Figure S3. Both complexes present a distorted octahedral geometry. The pyridine ligands are tilted at an angle larger than 40° with respect to the plane of the octahedron. The Ru–N bond length for the three ligands in both complexes (Table S2) decreases in the order py > bpy > dcbpy, reflecting the reduction of the donor character of the ligand and its increasing acceptor ability.

For both complexes, the LUMO orbital is located mainly on the dcbpy ligand, while for $(\mathbf{1})^{2+}$, the next orbital in energy is located on the bpy (Figures S4 and S5). The HOMO, H-1, and H-2 orbitals are the dπ orbitals centered on the ruthenium ion. (TD)DFT helps in the assignment of the observed transitions in the visible region. Figure 3 shows the energy and intensity of the predicted transitions and their comparison with the experimental results for $(\mathbf{1})^{2+}$ and $(\mathbf{2})^{2+}$ in acidic media. The lower-energy MLCT band in both complexes has the same origin, a transition from the dπ(Ru) orbital lower in energy (H-2) to the LUMO centered at the dcbpy (Figures S6 and S7, and Tables S4 and S5). The calculated spectrum for $(\mathbf{1})^{2+}$ reproduces well the presence of the extra MLCT at higher energy that corresponds to a π*(bpy)←dπ(Ru) transition.

The NMR spectra of basic solutions of $(\mathbf{1})^{2+}$ and $(\mathbf{2})^{2+}$ exposed to visible light (λ_{irr} = 450 nm) reveal the nature of the process responsible for the shorter lifetime of the excited state. Figure 4 shows the NMR spectra of a solution of $(\mathbf{2})^{2+}$ in an Na_2CO_3 (0.1 M) solution in D_2O before and after irradiation with 450 nm. Upon irradiation, the signals for the coordinated pyridine decrease and the signals for the free pyridine become apparent. Also several new signals are observed that correspond to the complex $[Ru(dcbpy)_2(py)(H_2O)]^{2+}$ ($\mathbf{2a}^{2+}$) (for a detailed assignment, see the Exp. Sect.).

The same experiment for $(\mathbf{1})^{2+}$ shows similar results, with the added complication that the product is an almost equimolar mixture of the two positional isomers of the complex $[Ru(dcbpy)(bpy)(py)(H_2O)]^{2+}$, $(\mathbf{1a})^{2+}$ and $(\mathbf{1a'})^{2+}$, where the py ligand is *trans* to the bpy or the dcbpy ligand, respectively (see Scheme 1 and Figure S8). In spite of this complication, it was possible to identify the signals for each isomer and quantify that they appear in a 1:1.1 ratio (see Figure S8 and the Exp. Sect. for the assignment). As the two isomers appear together, from now on we will refer to them collectively as $(\mathbf{1a})^{2+}$.

The above process can also be monitored in the visible spectra (Figure 5). Irradiation of basic solutions of $(\mathbf{1})^{2+}$ or $(\mathbf{2})^{2+}$ (λ_{irr} = 450 nm) results in a redshift in their MLCT maxima from 470 to 484 nm for $(\mathbf{1})^{2+}$, and from 478 to 489 nm for $(\mathbf{2})^{2+}$. Another significant change observed is the decrease of the intensity of the 374 nm band for $(\mathbf{1})^{2+}$ and 368 nm for $(\mathbf{2})^{2+}$. Three isosbestic points are observed for both systems, which is consistent with a

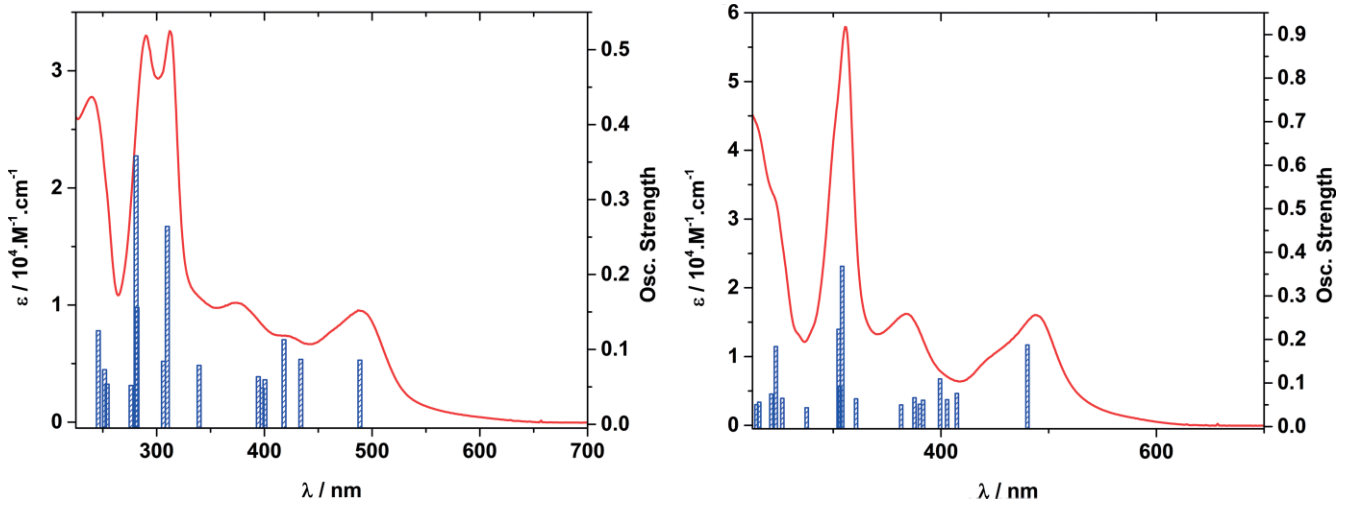

Figure 3. Comparison of the visible spectra and the energy of the transitions predicted by (TD)DFT calculations (bars) in acidic media of $(\mathbf{1})^{2+}$ (left) and $(\mathbf{2})^{2+}$ (right).

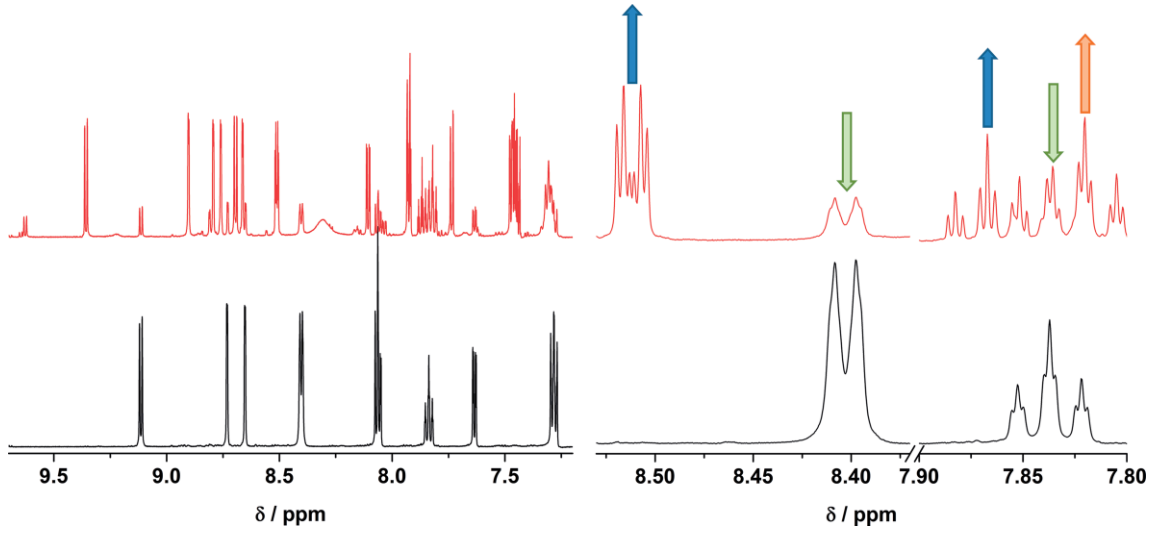

Figure 4. Changes in the ^{1}H NMR spectra of a solution of $(\mathbf{2})^{2+}$ in Na_2CO_3 (0.1 M) in D_2O before (black) and after (red) 5 min of irradiation with λ_{irr} = 450 nm. The blue arrows identify the peaks for the free py, the orange ones correspond to the coordinated py in $(\mathbf{2a})^{2+}$, while the green ones correspond to the coordinated py ligand in $(\mathbf{2})^{2+}$.

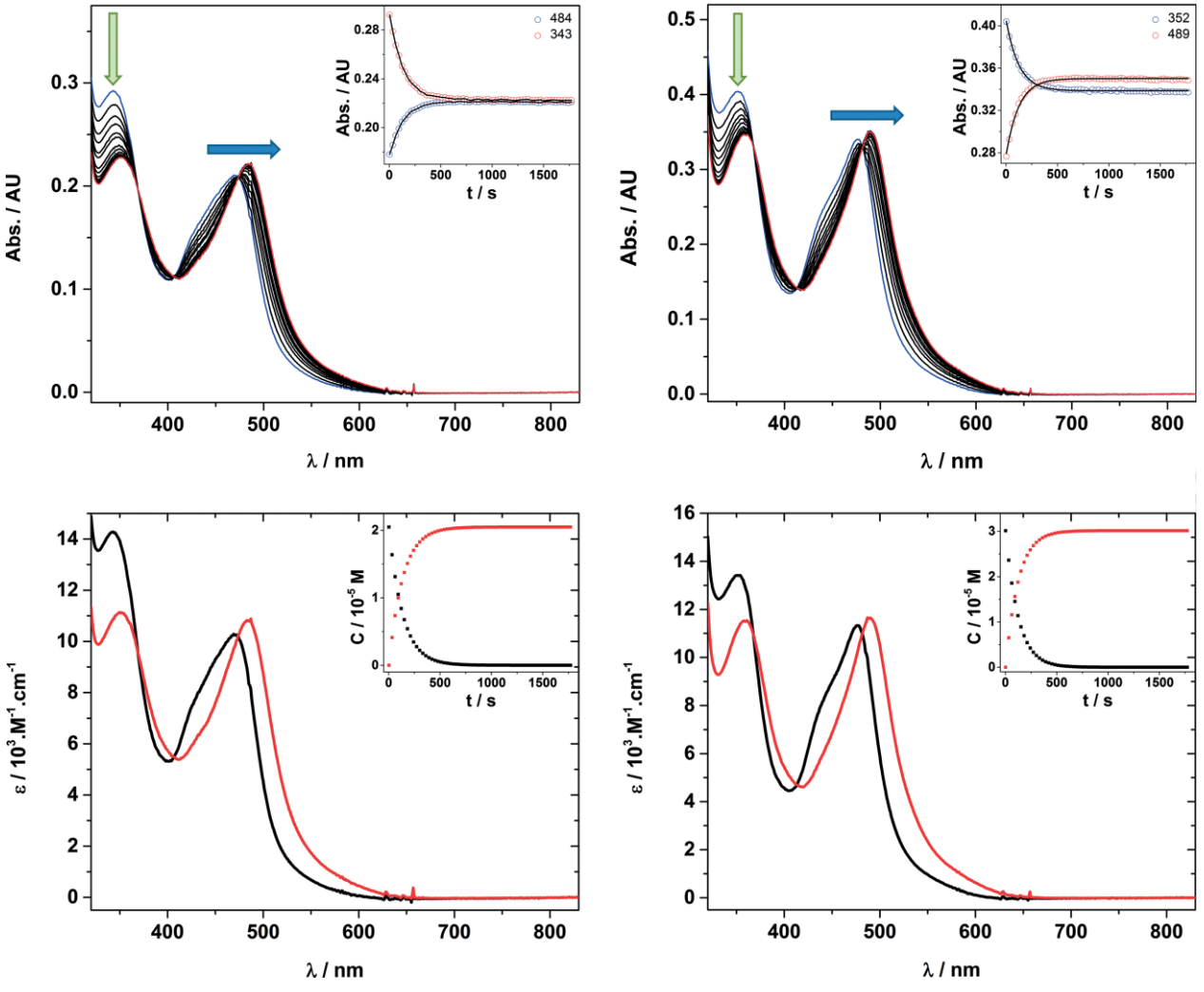

Figure 5. (Top) Changes in the electronic absorption spectra in basic media, with λ_{irr} = 450 nm for $(\mathbf{1})^{2+}$ (left) and $(\mathbf{2})^{2+}$ (right), for a total of t_{irr} = 1800 s. The insets show the evolution of the absorbance at two selected wavelengths, together with their fitting considering only one reaction. (Bottom) Spectra obtained in the fitting process for the two species. The insets show their concentration evolution.

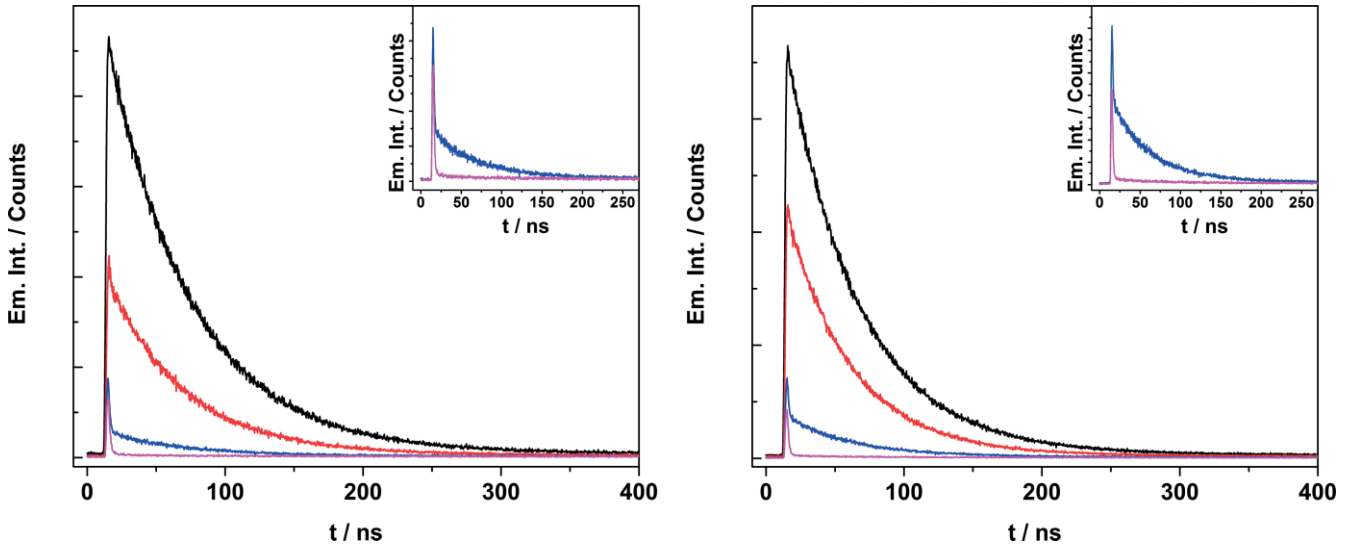

Figure 6. Emission decay for basic solutions of complexes $(\mathbf{1})^{2+}$ (left) and $(\mathbf{2})^{2+}$ (right) before (black) and after irradiation with λ_{irr} = 450 nm at different times: 2 min (red), 7 min (blue), and 20 min (pink). Insets show only the two longer irradiation times.

single dominant reaction in each process. The observed spectral changes are compatible with the same reaction identified in the NMR spectroscopic experiments, the substitution of a pyridine ligand by water to form $(\mathbf{1a})^{2+}$ or $(\mathbf{2a})^{2+}$. Irradiation of both complexes at the same wavelength under acidic conditions also leads to a redshift of the MLCT transition (Figure S9). However, in this case, the observed isosbestic points only hold at short times (t < 600 s), which indicates the onset of another process, the substitution of the remaining pyridine in $(\mathbf{1a})^{2+}$ or $(\mathbf{2a})^{2+}$ by water.

To obtain the quantum yield for the photosubstitution process on both complexes, we modeled the reaction considering only one process for the reactions in basic media and two consecutive steps for the reactions at low pH. The fitting procedure was very satisfactory, and the calculated traces reproduce well the observed behavior (Figures 5 and S7). This analysis allowed us not only to obtain the quantum yield for the photorelease of pyridine, but also the visible spectra of the photoproducts $(\mathbf{1a})^{2+}$ and $(\mathbf{2a})^{2+}$ in both media (Figures 5 and S9, and Table 1).

The photolysis of complexes $(\mathbf{1})^{2+}$ and $(\mathbf{2})^{2+}$ also has a strong impact on the emission properties of both complexes in each medium. For example, upon irradiation in the visible range of a basic solution of $(\mathbf{1})^{2+}$, its emission becomes weaker and its decay shows biexponential behavior, with a short lifetime component that is more pronounced upon extended times of irradiation (Figure 6). This behavior, also observed for $(\mathbf{2})^{2+}$, indicates that the products of the photolysis, $(\mathbf{1a})^{2+}$ and $(\mathbf{2a})^{2+}$, are weak emitters, as found for other Ru^{II}–aquo complexes.[36] The observed change in the emission properties of these complexes upon irradiation provides an alternative way to monitor the photolysis reaction when the reaction conditions preclude the use of visible absorption, as in a heterogeneous medium.

As these complexes could be the basis for a new family of cage compounds to be used in biological experiments, the temperature dependence of the quantum yield for the photoinduced substitution of the ligands is a property of great interest. Table S5 collects these values for complexes $(\mathbf{1})^{2+}$ and $(\mathbf{2})^{2+}$ in both aqueous media, and Figure 7 plots the inverse of the quantum yield in basic media for photosubstitution (φ_{PS}) as a function of 1/T, together with the best fit for the data using Equation (1) originally proposed by Durham et al.[37]

$$(\varphi_{PS})^{-1} = 1 + k_0 \exp(\Delta E_a/RT) \quad (1)$$

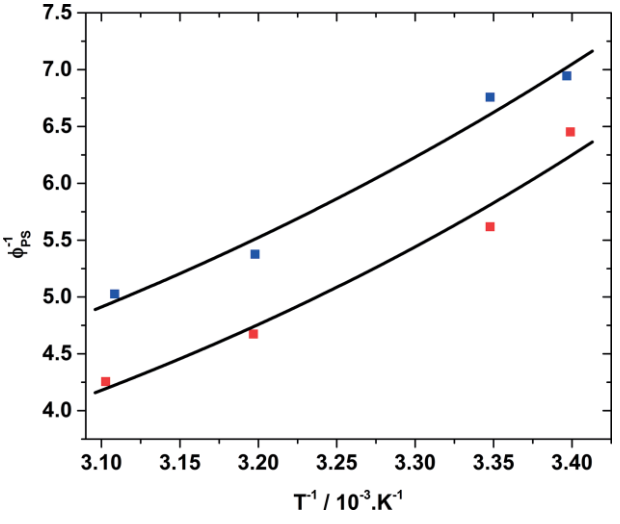

Figure 7. Plot of ϕ_{PS}^{-1} vs. T^{-1} for $(\mathbf{1})^{2+}$ (blue squares) and $(\mathbf{2})^{2+}$ (red squares). The line shows the best fitting to both data sets according to Equation (1).

For $(\mathbf{2})^{2+}$, the fit to Equation (1) is very satisfactory and gives an activation energy of 13.9 kJ/mol (1160 cm^{-1}). Fitting for $(\mathbf{1})^{2+}$ gives a similar, but smaller, activation energy of 12.1 kJ/mol (1010 cm^{-1}). Although the latter fitting is slightly less satisfactory, the result is surprisingly good, considering that the reaction consists actually of two simultaneous reactions that give two different photoproducts [$(\mathbf{1a})^{2+}$ and $(\mathbf{1a'})^{2+}$]. It should also be considered that $(\mathbf{1})^{2+}$ has two different chromophores, and this results in an additional ^{3}MLCT excited state of slightly

higher energy. This different electronic structure could lead to a more complex temperature dependence.

The observed temperature dependence is smaller than the one observed for $[Ru(bpy)_2PMe_3Glu]^+$ (Glu = glutamate),[3] but is still larger than the one reported for $[Ru(bpy)_2py_2]^{2+}$, where no temperature dependence of the quantum yield of photosubstitution was observed.[35]

For ruthenium–polypyridines, the presence of a ^{3}LF state lying at a higher energy than the emitting ^{3}MLCT is a well-established fact.[7] Its presence was first inferred from the temperature dependence of the quantum yield of the emission of $[Ru(bpy)_3]^{2+}$,[38] and a similar behavior has been observed for several related complexes. The presence of this state has also been explored using theoretical tools.[39,40] In most of the systems explored, the ^{3}LF state lies more than 3000 cm^{-1} above the ^{3}MLCT. This order can be altered by using sterically hindered ligands that lower the energy of the ^{3}LF state,[41,42] or by using ligands with higher-energy acceptor orbitals that increase the energy of the ^{3}MLCT.[43] Both strategies lead to the detection of the ^{3}LF state in transient absorption experiments, either by its role in the dynamics of the decay of the ^{3}MLCT state[41,42] or by direct spectroscopic observation.[43]

The energy of activation reported for the photosubstitution process[12,26] is much smaller than the energy gap between the ^{3}MLCT and the ^{3}LF states evaluated from the emission measurements on systems with chelate ligands, where the photosubstitution is much less prominent. Theoretical calculations have shown that elongation of the Ru–L distance is involved in the pathway leading to the ^{3}LF state. Also the participation of a second ^{3}LF has been proposed.[44] These proposed pathways require the elongation of the monodentate ligand and probably contribute to the smaller activation energy observed. Interestingly, although the cage compound $[Ru(bpy)_2PMe_3Glu]^{2+}$ has its absorption maxima blueshifted compared with $(\mathbf{1})^{2+}$ and $(\mathbf{2})^{2+}$, it has a higher activation energy for the photosubstitution process. This is probably related to the higher binding energy of the Ru–P bond that has to be weakened in the activated complex, leading to the photosubstitution products.

The role of the energy gap between ^{3}MLCT and the ^{3}LF also provides an explanation for the low quantum yield for the photosubstitution reaction observed for $(\mathbf{1})^{2+}$ and $(\mathbf{2})^{2+}$ at low pH. The protonation of the dcbpy ligand results in a stabilization of the LUMO and a lower energy for the ^{3}MLCT, as expressed by the redshift of the energy of the emission maxima. So, in this case, the energy gap between the ^{3}MLCT and the ^{3}LF state is much larger, and this leads to a lower quantum yield for the photosubstitution reaction and a longer emission lifetime.

Conclusion

The complexes $(\mathbf{1})^{2+}$ and $(\mathbf{2})^{2+}$ have been shown to be very active for the photosubstitution of a pyridine ligand at physiological pH, and by extension, it should be a very useful fragment for the caging of molecules containing functionalities like nitriles and amines, as has been found for complexes of the family $[Ru(bpy)_2L_2]^{2+}$. This behavior is due to the presence of a deprotonated form of the dcbpy ligand that increases the energy of the ^{3}MLCT state and opens the thermal population of the ^{3}LF state responsible for the photoinduced substitution of pyridine. Interestingly, the protonated form is much less active, due to the stabilization of the ^{3}MCLT state brought by the protonated carboxylic group. This suggests that the inclusion of deprotonable carboxylates is a viable strategy to increase the activity of a given bpy-based cage compound at physiological pH. The inclusion of this group will also have the benefit of increasing the solubility of the cage in water at physiological pH. On the contrary, an ester group on the bpy ligand would result in a lower-energy ^{3}MLCT state that will be less effective in populating the ^{3}LF state, and it should present a lower quantum yield for the photosubstitution reaction.

Experimental Section

Materials: The solvents used were of HPLC quality and were previously dried, when needed, according to published procedures,[45] and deoxygenated by freeze–pump–thaw processes or argon bubbling.

Synthesis: The ligands 4,4′-dicarboxy-2,2′-bipyridine (dcbpy)[46] and 4,4′-bis(methoxycarbonyl)-2,2′-bipyridine (dmebpy),[47] and the complexes *cis*-$[Ru(DMSO)_4Cl_2]$,[48] *cis*,*cis*-$Ru(bpy)(DMSO)_2Cl_2$,[30] *cis*-$Ru(bpy)_2Cl_2$,[49] *cis*-$Ru(dcbpy)_2Cl_2$,[31] $[Ru(bpy)_2(dcbpy)](PF6)_2$,[34] and $[Ru(bpy)(dcbpy)_2](PF_6)_2$,[50] were prepared according to previously reported procedures. All other reagents were commercially available (Sigma–Aldrich) and were used without further purification. All the compounds were vacuum-dried with silica gel for at least 12 h, prior to characterization.

$Ru(bpy)(dmebpy)Cl_2$: Dry methanol (200 mL) was deoxygenated by argon bubbling (60 min) in a Schlenk flask. The compound *cis*,*cis*-$Ru(bpy)(DMSO)_2Cl_2$ (403.0 mg, 0.8319 mmol, M_r = 484.43), the dmebpy ligand (225.6 mg, 0.8286 mmol, M_r = 272.26), and LiCl (701.9 mg, 16.56 mmol, M_r = 42.39) were added to the deoxygenated solvent, against an argon stream. The resulting orange-colored suspension was heated to reflux under argon. After 18 h, the reaction mixture was cooled to room temperature and was then vacuum-concentrated (at 35 °C) to complete dryness. The resulting solid was resuspended in distilled water (5 mL), obtaining a deep-orange solution and a purple microcrystalline powder, which was further washed with cold water and diethyl ether. The obtained product was placed in the desiccator for 48 h. Purity was confirmed by thin-layer chromatography (silica gel; running solvent: acetone/methanol, 9:1). The solid was recrystallized from dichloromethane by diethyl ether addition, obtaining the final product (195.0 mg, 0.3153 mmol, M_r = 618.43). Yield: 37.9 %. $Ru(bpy)(dmebpy)Cl_2{\cdot}H_2O$ (618.43 g mol^{-1}): calcd. C 46.6, H 3.6, N 9.1; found C 46.3, H 3.8, N 8.7. $Ru(bpy)(dmebpy)Cl_2$ (see Scheme S1). ^{1}H NMR [500.13 MHz, Na_2CO_3 (0.1 M) in D_2O]: δ = 10.200 (dd, J = 6.5/0.5 Hz, 1 H, A-H), 8.204 (dd, J = 6.0/1.5 Hz, 1 H, B-H), 9.087 (d, J = 1.5 Hz, 1 H, C-H), 7.878 (dd, J = 6.0/0.5 Hz, 1 H, A′-H), 7.520 (dd, J = 6.5/1.5 Hz, 1 H, B′-H), 8.913 (d, J = 1.5 Hz, 1 H, C′-H), 9.864 (ddd, J = 6.0/1.0/–Hz, 1 H, 1-H), 7.835 (ddd, J = 8.0/6.0/1.0 Hz, 1 H, 2-H), 8.158 (ddd, J = 8.0/8.0/1.5 Hz, 1 H, 3-H), 8.701 (d, J = 8.0 Hz, 1 H, 4-H), 7.388 (ddd, J = 6.0/1.0/– Hz, 1 H, 1′-H), 7.107 (ddd, J = 7.5/6.0/1.5 Hz, 1 H, 2′-H), 7.772 (ddd, J = 8.0/7.5/1.5 Hz, 1 H, 3′-H), 8.539 (d, J = 8.0 Hz, 1 H, 4′-H), 4.040 (s, 3 H, 6-H), 3.884 (s, 3, D′-H) ppm.

$[Ru(bpy)(dcbpy)(py)_2](PF_6)_2$ $(\mathbf{1})(PF_6)_2$: Previously distilled pyridine (800 µL, 782 mg, 9.9 mmol; ϱ = 0.978 g mL^{-1}; M_r = 79.10) was added

to milliQ water (5 mL). The mixture was deoxygenated with argon by a freeze–pump–thaw process. $Ru(bpy)(dmebpy)Cl_2 \cdot H_2O$ (54.1 mg, 0.0875 mmol, M_r = 618.43) was added to this mixture, against an argon stream, and it was heated to reflux under argon, with constant stirring, while covered with aluminium foil. After 4 h, Na_2CO_3 (204.0 mg, 1.925 mmol, M_r = 105.99) was added and the heating continued for another 30 min. Then the solution was cooled to room temperature, filtered to remove any undesired solid, and then vacuum-concentrated (at 35 °C) to complete dryness. The residue was washed with diethyl ether to remove excess pyridine (4 × 10 mL) and was resuspended in anhydrous methanol, filtering off the excess sodium carbonate. The deep-orange solution obtained was vacuum-concentrated (at 35 °C) to complete dryness. The residue was dissolved in HCl (0.5 M, 3 mL), and this solution was added dropwise to an NH_4PF_6 solution (60.0 mg NH_4PF_6, 0.3681 mmol, M_r = 163.00, in 0.5 mL of milliQ water). This suspension was allowed to settle in a refrigerator for 24 h. The red-brown solid thus obtained was filtered and washed with the minimum amount of cold distilled water. The product was recrystallized from acetone by the addition of diethyl ether, obtaining a deep-orange solid (75.0 mg, 0.073 mmol, M_r = 1021.65). Yield: 29.0 %. $[Ru(bpy)(dcbpy)(py)_2](PF_6)_2 \cdot 4H_2O$ (1021.65 g mol^{-1}): calcd. C 37.6, H 3.4, N 8.2; found C 37.5, H 3.0, N 8.2. Compound $(\mathbf{1})^{2+}$ (see Scheme S1). ^{1}H NMR [500.13 MHz, Na_2CO_3 (0.1 M) in D_2O]: δ = 9.116 (d, J = 6.0 Hz, 1 H, A-H), 8.043 (dd, J = 6.0/1.5 Hz, 1 H, B-H), 8.721 (d, J = 1.5 Hz, 1 H, C-H), 8.093 (d, J = 6.0 Hz, 1 H, A′-H), 7.625 (dd, J = 6.0/1.5 Hz, 1 H, B′-H), 8.645 (d, J = 1.5 Hz, 1 H, C′-H), 9.022 (dd, J = 5.5/1.0 Hz, 1 H, 1-H), 7.765 (ddd, J = 7.0/5.5/1.0 Hz, 1 H, 2-H), 8.138 (ddd, J = 8.0/8.0/1.5 Hz, 1 H, 3-H), 8.393 (d, J = 8.0 Hz, 1 H, 4-H), 7.952 (dd, J = 5.5/1.0 Hz, 1 H, 1′-H), 7.324 (ddd, J = 7.5/6.0/1.5 Hz, 1 H, 2′-H), 7.909 (ddd, J = 7.5/7.5/1.5 Hz, 1 H, 3′-H), 8.304 (d, J = 8.0 Hz, 1 H, 4′-H), 8.418 (d, J = 6.0 Hz, 2 H, 5-H), 7.284 (dd, J = 6.0/1.0 Hz, 2 H, 6-H), 7.839 (tt, J = 8.0/1.5 Hz, 1 H, 7-H) ppm, 8.408 (d, J = 6.0 Hz, 2 H, 8-H), 7.270 (dd, J = 6.5/1.0 Hz, 2 H, 9-H), 7.824 (tt, J = 8.0/1.5 Hz, 1 H, 10-H) ppm. Compound $(\mathbf{1a})^{2+}$ (see Scheme S1). ^{1}H NMR [500.13 MHz, Na_2CO_3 (0.1 M) in D_2O]: δ = 9.370 (d, J = 6.0 Hz, 1 H, A-H), 8.090 (dd, J = 6.0/1.5 Hz, 1 H, B-H), 8.767 (d, J = 1.5 Hz, 1 H, C-H), 7.957 (d, J = 6.0 Hz, 1 H, E-H), 7.443 (dd, J = 6.0/1.5 Hz, 1 H, F-H), 8.636 (d, J = 1.5 Hz, 1 H, G-H), 8.599 (d, J = 5.0 Hz, 1 H, 1-H), 7.633 (ddd, J = 7.5/5.5/1.0 Hz, 1 H, 2-H), 8.149 (ddd, J = 7.5/7.5/1.0 Hz, 1 H, 3-H), 8.560 (d, J = 7.5 Hz, 1 H, 4-H), 7.623 (d, J = 5.5 Hz, 1 H, 5-H), 7.159 (ddd, J = 7.5/6.0/1.0 Hz, 1 H, 6-H), 7.840 (ddd, J = 8.0/8.0/1.0 Hz, 1 H, 7-H), 8.407 (d, J = 8.0 Hz, 1 H, 8-H), 8.340 (–, –, –, 9-H), 7.308 (–, –, 2 H, 10-H), 7.823 (–, –, 1 H, 11-H) ppm. Compound $(\mathbf{1a'})^{2+}$ (see Scheme S1). ^{1}H NMR [500.13 MHz, Na_2CO_3 (0.1 M) in D_2O]: δ = 8.724 (d, J = 6.0 Hz, 1 H, A-H), 7.914 (dd, J = 6.0/1.5 Hz, 1 H, B-H), 8.885 (d, J = 1.5 Hz, 1 H, C-H), 7.797 (d, J = 6.0 Hz, 1 H, E-H), 7.464 (dd, J = 6.0/1.5 Hz, 1 H, F-H), 8.743 (d, J = 1.5 Hz, 1 H, G-H), 9.279 (d, J = 5.0 Hz, 1 H, 1-H), 7.809 (ddd, J = 8.0/5.0/1.0 Hz, 1 H, 2-H), 8.122 (ddd, J = 8.0/8.0/1.0 Hz, 1 H, 3-H), 8.429 (d, J = 7.5 Hz, 1 H, 4-H), 7.789 (–, –, 1 H, 5-H), 7.147 (ddd, J = 7.5/5.0/1.0 Hz, 1 H, 6-H), 7.775 (ddd, J = 8.0/8.0/1.0 Hz, 1 H, 7-H), 8.293 (d, J = 8.0 Hz, 1 H, 8-H), 8.330 (–, –, –, 9-H), 7.294 (–, –, 2 H, 10-H), 7.807 (–, –, 1 H, 11-H) ppm.

$[Ru(dcbpy)_2(py)_2](PF_6)_2$ (2)$(PF_6)_2$: Previously distilled pyridine (800 µL, 782 mg, 9.9 mmol, ϱ = 0.978 g mL^{-1}, M_r = 79.10) was added to milliQ water (3 mL). The mixture was deoxygenated with argon by a freeze–pump–thaw process. The compound *cis*-$Ru(dcbpy)_2Cl_2$ (130.2 mg, 0.197 mmol, M_r = 660.38) was added to this mixture, against an argon stream. The resulting mixture was heated to reflux under argon with constant stirring, while covered with aluminium foil. After refluxing for 6.5 h, the solution was cooled to room temperature, filtered to remove any undesired solid, and then vacuum-concentrated (at 35 °C) to complete dryness. The residue was washed with cyclohexane to remove excess pyridine (3 × 30 mL). The solid thus obtained was dissolved in the minimum volume of Na_2CO_3 (0.1 M) solution, and precipitated by the addition of a stoichiometric amount of KPF_6, followed by dropwise addition of HCl (1 M). This suspension was allowed to settle in a refrigerator for 24 h. The red-brown solid thus obtained was filtered and washed with a minimum amount of cold distilled water, obtaining the final product (115.7 mg, 0.0985 mmol, M_r = 1174.27). Yield: 50.0 %. $[Ru(dcbpy)_2(py)_2](PF_6)_2 \cdot 1.5H_2O \cdot 1.5DMF$ (1174.27 g mol^{-1}): calcd. C 39.4, H 3.4, N 8.9; found C 39.3, H 3.2, N 9.1. Compound $(\mathbf{2})^{2+}$ (see Scheme S1). ^{1}H NMR [500.13 MHz, Na_2CO_3 (0.1 M) in D_2O]: δ = 9.115 (d, J = 5.5 Hz, 2 H, A-H), 8.056 (dd, J = 6.0/1.5 Hz, 2 H, B-H), 8.733 (d, J = 1.5 Hz, 2 H, C-H), 8.070 (d, J = 6.0 Hz, 2 H, A′-H), 7.635 (dd, J = 6.0/1.5 Hz, 2 H, B′-H), 8.653 (d, J = 1.5 Hz, 2 H, C′-H), 8.403 (d, J = 5.5 Hz, 4 H, 1-H), 7.283 (ddd, J = 7.0/5.5/1.5 Hz, 4 H, 2-H), 7.837 (tt, J = 7.0/7.0/1.5/1.5 Hz, 2 H, 3-H) ppm. Compound $(\mathbf{2a})^{2+}$ (see Scheme S1). ^{1}H NMR [500.13 MHz, Na_2CO_3 (0.1 M) in D_2O]: δ = 8.695 (dd, J = 6.0/0.5 Hz, 1 H, A-H), 7.923 (dd, J = 6.0/2.0 Hz, 1 H, B-H), 8.904 (d, J = 1.5 Hz, 1 H, C-H), 7.736 (dd, J = 6.0/0.5 Hz, 1 H, A′-H), 7.472 (dd, J = 6.0/2.0 Hz, 1 H, B′-H), 8.760 (d, J = 1.0 Hz, 1 H, C′-H), 9.357 (dd, J = 6.0/0.5 Hz, 1 H, E-H), 8.106 (dd, J = 6.0/1.5 Hz, 1 H, F-H), 8.794 (d, J = 1.5 Hz, 1 H, G-H), 7.927 (dd, J = 6.0/0.5 Hz, 1 H, E′-H), 7.453 (dd, J = 6.0/1.5 Hz, 1 H, F′-H), 8.664 (d, J = 1.5 Hz, 1 H, G′-H), 8.307 (–, –, 2 H, 1-H), 7.306 (–, J = 7.5/–/– Hz, 2 H, 2-H), 7.820 (tt, J = 7.5/1.5 Hz, 1 H, 3-H) ppm.

Methods: Elemental analysis of C, H, and N was performed with a Carlo Erba 1108 analyzer on our institute. The ^{1}H NMR and COSY spectra were obtained at 25 °C with a Bruker ARX500 spectrometer, with an operating frequency of 500.13 MHz for ^{1}H. Solutions of commercially available deuterated solvents (ca. 10 mM, Sigma–Aldrich) were used. All spectra were referenced to TMS (tetramethylsilane) using solvent residual peaks as an internal standard, and were processed using MestReNova software, version 6.2.1-7569. For photosubstitution experiments monitored by this technique, the samples were irradiated inside the NMR spectroscopy tubes, using an LED source with λ_{irr} = 450 nm. Irradiation was performed at 1 min intervals, with homogenization of the sample between intervals. UV/Vis absorption spectroscopy measurements were obtained with a Hewlett–Packard 8453 spectrophotometer with a diode arrangement within a 190–1100 nm range. All spectra were taken with a standard integration time of 0.5 s, using dry solvents and quartz glass cuvettes with a 1.00 cm optical path length. Spectra at fixed pH were measured in buffer solutions of pH 1.1 [HCl (0.1 M)] and pH 7.4 [NaH_2PO_4/Na_2HPO_4 (0.1 M)].[51] The system was thermostatted prior to every measurement, using a custom-built holder. The holder was liquid-cooled, and was connected to a cryostat Lauda RC6 that also permitted irradiation perpendicular to the measurement direction. For photosubstitution experiments, the sample was irradiated in a fluorescence quartz cuvette with a 1.00 cm × 1.00 cm optical path length, with a screw cap, under constant stirring. Irradiation was performed with an LED source at 450 nm, $I_0 = 2.70 \times 10^{-6}$ einstein s^{-1} L^{-1}, placed at 90° with respect to the absorption measurement direction.

Photoreactivity Studies: The photosubstitution process monitored by UV/Vis absorption spectroscopy was analyzed by using multivariate analysis, with an approach similar to the one used for chemical-equilibrium studies.[52] For this purpose, a fitting routine, developed by the group of Dr. Leonardo D. Slep in Octave,[53] was used. This procedure was developed and used in Dr. Juan P. Marcolongo's doctoral thesis,[54] and will be published elsewhere in the near future. For analysis implementation, the initial reagent concentration and

a reaction model (differential equations) were needed. Calibration of the experimental setup was performed by using $[Ru(bpy)_2(ACN)_2](PF_6)_2$ as an actinometer.[55]

Photophysical Studies: Steady-state emission was measured with a PTI-Quantamaster 40 fluorometer, at 25 °C, in argon-saturated solutions. Quantum yields were calculated using $[Ru(bpy)_3]^{2+}$ (φ = 0.063 in H_2O at 25 °C) as reference.[56] Emission and excitation slits were fixed at 4 nm, and the scanning speed was 3 nm seg^{-1}, to minimize undesired photolysis upon irradiation. Emission- and excitation-correction functions provided by the manufacturer were used. For the photosubstitution experiments monitored by this technique, the samples were irradiated using the same experimental array as for the UV/Vis absorption spectroscopy experiments, using fixed irradiation time intervals, and then measuring the emission in the same way as for non-irradiated complexes. Photoluminescence decay measurements were performed by irradiating at 450 nm and collecting the emitted light from 500 to 900 nm, selected through an interference filter. The collection time was 120 s. The source used was a laser diode, which generated light pulses of 450 nm with a full width at half maximum of 1.4 ns and 640 ns, with a 1.1 μs time window between pulses. Emission was collected using a lens of numeric aperture 0.3 directed through the interference filter, and focused on the detector. The signal was recorded with an avalanche photodiode and a single-photon counting board. For the photosubstitution experiments monitored by this technique, the samples were irradiated using the same experimental array as for UV/Vis absorption spectroscopy experiments, using fixed irradiation time intervals, and then measuring the photoluminescence decay in the same way as for non-irradiated complexes.

Theoretical Calculations: In this work, density functional theory calculations were used to optimize the geometries for the two informed complexes in acidic aqueous media. Solvation effects were taken into account using the last implementation of the implicit solvation model IEF-PCM.[57–59] Calculations were performed with the Gaussian 09 package,[60] using the B3LYP functional. In every case, we employed the LanL2DZ effective-nucleus-potential basis set,[61–63] which has been proven to be appropriate for geometry prediction in coordination compounds containing metal atoms from the second-transition series of the Periodic Table. SCF strict convergence criteria were used, along with the default options in geometry optimization and IR, and every optimized structure was confirmed by analysis of the minima of the harmonic vibrational frequencies.[64] Energies and intensities for vertical electronic transitions were evaluated using the time-dependent DFT (TD-DFT) approach[65,66] with the Gaussian 09[60] package, and the isodensity plots for the orbitals involved in these transitions were visualized using GaussView 5.[67] GaussSum[68] software was used to perform spectral simulations and to extract information of the molecular orbitals.

Acknowledgments

This work was partially supported by the University of Buenos Aires (UBACyT q643 and UBACyT q534), CONICET (PIP 0659) and ANPCyT (PICT 2013 0029 and PICT 2012 2041). L. B. V. and J. H. H. are members of the scientific staff of CONICET, and R. C. acknowledges fellowship support from the same institution. The authors thank Dr. L. D. Slep, Dr. J. P. Marcolongo, and J. Schmidt for their help implementing spectral fitting using Octave, and for useful discussions. P. R. thanks Dr. G. E. Pieslinger for his help with the DFT calculations.

Keywords: Photosubstitution · Ruthenium · Photochemistry · Temperature-dependent quantum yield · Carboxylate ligands

[1] J. D. Knoll, C. Turro, *Coord. Chem. Rev.* **2015**, *282–283*, 110–126.
[2] I. Romero-Canelón, P. J. Sadler, *Inorg. Chem.* **2013**, *52*, 12276–12291.
[3] L. Zayat, O. Filevich, L. M. Baraldo, R. Etchenique, *Philos. Trans. R. Soc. A* **2013**, *371*, 20120330.
[4] V. Balzani, G. Bergamini, P. Ceroni, *Coord. Chem. Rev.* **2008**, *252*, 2456–2469.
[5] M. Grätzel, *Acc. Chem. Res.* **2009**, *42*, 1788–1798.
[6] D. L. Ashford, M. K. Gish, A. K. Vannucci, M. K. Brennaman, J. L. Templeton, J. M. Papanikolas, T. J. Meyer, *Chem. Rev.* **2015**, *115*, 13006–13049.
[7] J. K. White, R. H. Schmehl, C. Turro, *Inorg. Chim. Acta* **2017**, *454*, 7–20.
[8] T. J. Meyer, *Pure Appl. Chem.* **1986**, *58*, 1193–1206.
[9] C. Brieke, F. Rohrbach, A. Gottschalk, G. Mayer, A. Heckel, *Angew. Chem. Int. Ed.* **2012**, *51*, 8446–8476; *Angew. Chem.* **2012**, *124*, 8572.
[10] L. Zayat, C. Calero, P. Alborés, L. M. Baraldo, R. Etchenique, *J. Am. Chem. Soc.* **2003**, *125*, 882–883.
[11] E. Ruggiero, S. Alonso-de Castro, A. Habtemariam, L. Salassa, *Struct. Bonding* **2015**, *165*, 69–108.
[12] See ref.[3]
[13] V. Nikolenko, R. Yuste, L. Zayat, L. M. Baraldo, R. Etchenique, *Chem. Commun.* **2005**, *44*, 1752–1754.
[14] L. Zayat, M. J. Salierno, R. Etchenique, *Inorg. Chem.* **2006**, *45*, 1728–1731.
[15] L. Zayat, M. G. Noval, D. J. Calvo, R. Etchenique, J. Campi, C. I. Calero, *ChemBioChem* **2007**, *8*, 2035–2038.
[16] M. J. Salierno, E. Marceca, D. S. Peterka, R. Yuste, R. Etchenique, *J. Inorg. Biochem.* **2010**, *104*, 418–22.
[17] O. Filevich, M. Salierno, R. Etchenique, *J. Inorg. Biochem.* **2010**, *104*, 1248–1251.
[18] R. Araya, V. Andino-Pavlovsky, R. Yuste, R. Etchenique, *ACS Chem. Neurosci.* **2013**, *4*, 1163–1167.
[19] R. N. Garner, J. C. Gallucci, K. R. Dunbar, C. Turro, *Inorg. Chem.* **2011**, *50*, 13–15.
[20] T. Respondek, R. N. Garner, M. K. Herroon, I. Podgorski, C. Turro, J. J. Kodanko, *J. Am. Chem. Soc.* **2011**, *133*, 17164–17167.
[21] H. Chan, J. B. Ghrayche, J. Wei, A. K. Renfrew, *Eur. J. Inorg. Chem.* **2016**, 1679–1686.
[22] M. K. Brennaman, R. J. Dillon, L. Alibabaei, M. K. Gish, C. J. Dares, D. L. Ashford, R. L. House, G. J. Meyer, J. M. Papanikolas, T. J. Meyer, *J. Am. Chem. Soc.* **2016**, *138*, 13085–13102.
[23] C. N. Fleming, K. A. Maxwell, J. M. DeSimone, T. J. Meyer, J. M. Papanikolas, *J. Am. Chem. Soc.* **2001**, *123*, 10336–10347.
[24] E. Terpetschnig, H. Szmacinski, H. Malak, J. R. Lakowicz, *Biophys. J.* **1995**, *68*, 342–50.
[25] P. Qu, D. W. Thompson, G. J. Meyer, *Langmuir* **2000**, *16*, 4662–4671.
[26] D. V. Pinnick, B. Durham, *Inorg. Chem.* **1984**, *23*, 3841–3842.
[27] D. V. Pinnick, B. Durham, *Inorg. Chem.* **1984**, *23*, 1440–1445.
[28] W. F. Wacholtz, R. A. Auerbach, R. H. Schmehl, *Inorg. Chem.* **1986**, *25*, 227–234.
[29] D. P. Rillema, C. B. Blanton, R. J. Shaver, D. C. Jackman, M. Boldaji, S. Bundy, L. Worl, T. J. Meyer, *Inorg. Chem.* **1992**, *31*, 1600–1606.
[30] M. Toyama, K. Inoue, S. Iwamatsu, N. Nagao, *Bull. Chem. Soc. Jpn.* **2006**, *79*, 1525–1534.
[31] M. K. Nazeeruddin, S. M. Zakeeruddin, R. Humphry-Baker, M. Jirousek, P. Liska, N. Vlachopoulos, V. Shklover, C.-H. Fischer, M. Grätzel, *Inorg. Chem.* **1999**, *38*, 6298–6305.
[32] J. Ferguson, A. W.-H. Mau, W. H. F. Sasse, *Chem. Phys. Lett.* **1979**, *68*, 21–24.
[33] M. K. Nazeeruddin, K. Kalyanasundaram, *Inorg. Chem.* **1989**, *28*, 4251–4259.
[34] R. M. O'Donnell, R. N. Sampaio, G. Li, P. G. Johansson, C. L. Ward, G. J. Meyer, *J. Am. Chem. Soc.* **2016**, *138*, 3891–3903.
[35] W. M. Wacholtz, R. A. Auerbach, R. H. Schmehl, M. Ollino, W. R. Cherry, *Inorg. Chem.* **1985**, *24*, 1758–1760.
[36] J. T. Hewitt, J. J. Concepcion, N. H. Damrauer, *J. Am. Chem. Soc.* **2013**, *135*, 12500–12503.
[37] B. Durham, J. V. Caspar, J. K. Nagle, T. J. Meyer, *J. Am. Chem. Soc.* **1982**, *104*, 4803–4810.

[38] J. Van Houten, R. J. Watts, *Inorg. Chem.* **1978**, *17*, 3381–3385.
[39] J. Bossert, C. Daniel, *Coord. Chem. Rev.* **2008**, *252*, 2493–2503.
[40] E. Borfecchia, C. Garino, L. Salassa, T. Ruiu, D. Gianolio, X. Zhang, K. Attenkofer, L. X. Chen, R. Gobetto, P. J. Sadler, C. Lamberti, *Dalton Trans.* **2013**, *42*, 6564–71.
[41] Q. Sun, S. Mosquera-Vazquez, L. M. Lawson Daku, L. Guénée, H. A. Goodwin, E. Vauthey, A. Hauser, *J. Am. Chem. Soc.* **2013**, *135*, 13660–13663.
[42] Q. Sun, S. Mosquera-Vazquez, Y. Suffren, J. Hankache, N. Amstutz, L. M. Lawson Daku, E. Vauthey, A. Hauser, *Coord. Chem. Rev.* **2015**, *282–283*, 87–99.
[43] A. Cadranel, G. E. Pieslinger, P. Tongying, M. K. Kuno, L. M. Baraldo, J. H. Hodak, *Dalton Trans.* **2016**, *45*, 5464–5475.
[44] M. R. Camilo, C. R. Cardoso, R. M. Carlos, a. B. P. Lever, *Inorg. Chem.* **2014**, *53*, 3694–3708.
[45] W. L. F. Armarego, D. D. Perrin, *Purification of Laboratory Chemicals*, Butterworth-Heinemann, Oxford, **1996**.
[46] K.-Y. Liu, C.-L. Hsu, S.-H. Chang, J.-G. Chen, K.-C. Ho, K.-F. Lin, *J. Polym. Sci., Part A: Polym. Chem.* **2010**, *48*, 366–372.
[47] B. D. Hosangadi, R. H. Dave, *Tetrahedron Lett.* **1996**, *37*, 6375–6378.
[48] I. Evans, A. Spencer, *J. Chem. Soc., Dalton Trans.* **1973**, 204–209.
[49] C. Viala, C. Coudret, *Inorg. Chim. Acta* **2006**, *359*, 984–989.
[50] H. Park, E. Bae, J.-J. Lee, J. Park, W. Choi, *J. Phys. Chem. B* **2006**, *110*, 8740–8749.
[51] R. M. C. Dawson, D. C. Elliott, W. H. Elliott, K. M. Jones, *Data for Biochemical Research*, Oxford University Press, Oxford, **1989**.
[52] M. Kubista, R. Sjoback, B. Albinsson, *Anal. Chem.* **1993**, *65*, 994–998.
[53] R. W. John W. Eaton, David Bateman, Søren Hauberg, **2016**.
[54] J. P. Marcolongo, J. Schmidt, N. Levin, L. D. Slep, *Phys. Chem. Chem. Phys.*, https://doi.org/10.1039/C7CP03619A.
[55] See ref.[27]
[56] A. M. Brouwer, *Pure Appl. Chem.* **2011**, *83*, 2213–2228.
[57] G. Scalmani, M. J. Frisch, *J. Chem. Phys.* **2010**, *132*, 114110.
[58] J. Tomasi, B. Mennucci, R. Cammi, *Chem. Rev.* **2005**, *105*, 2999–3093.
[59] S. Miertuš, E. Scrocco, J. Tomasi, *Chem. Phys.* **1981**, *55*, 117–129.
[60] M. J. Frisch, G. W. Trucks, H. B. Schlegel, G. E. Scuseria, M. A. Robb, J. R. Cheeseman, J. A. Montgomery, Jr., T. Vreven, K. N. Kudin, J. C. Burant, J. M. Millam, S. S. Iyengar, J. Tomasi, V. Barone, B. Mennucci, M. Cossi, G. Scalmani, N. Rega, G. A. Petersson, H. Nakatsuji, M. Hada, M. Ehara, K. Toyota, R. Fukuda, J. Hasegawa, M. Ishida, T. Nakajima, Y. Honda, O. Kitao, H. Nakai, M. Klene, X. Li, J. E. Knox, H. P. Hratchian, J. B. Cross, V. Bakken, C. Adamo, J. Jaramillo, R. Gomperts, R. E. Stratmann, O. Yazyev, A. J. Austin, R. Cammi, C. Pomelli, J. W. Ochterski, P. Y. Ayala, K. Morokuma, G. A. Voth, P. Salvador, J. J. Dannenberg, V. G. Zakrzewski, S. Dapprich, A. D. Daniels, M. C. Strain, O. Farkas, D. K. Malick, A. D. Rabuck, K. Raghavachari, J. B. Foresman, J. V. Ortiz, Q. Cui, A. G. Baboul, S. Clifford, J. Cioslowski, B. B. Stefanov, G. Liu, A. Liashenko, P. Piskorz, I. Komaromi, R. L. Martin, D. J. Fox, T. Keith, M. A. Al-Laham, C. Y. Peng, A. Nanayakkara, M. Challacombe, P. M. W. Gill, B. Johnson, W. Chen, M. W. Wong, C. Gonzalez, J. A. Pople, *Gaussian 03*, revision C.01, Gaussian, Inc., Wallingford, CT, **2004**.
[61] W. R. Wadt, P. J. Hay, *J. Chem. Phys.* **1985**, *82*, 284–298.
[62] P. J. Hay, W. R. Wadt, *J. Chem. Phys.* **1985**, *82*, 270.
[63] T. H. Dunning Jr., P. J. Hay in *Modern Theoretical Chemistry*, vol. 3 (Ed.: H. Schaefer III), Plenum, New York, **1976**, pp. 1–25.
[64] H. B. Schlegel, *J. Comput. Chem.* **1982**, *3*, 214–218.
[65] L. Petit, P. Maldivi, C. Adamo, *J. Chem. Theory Comput.* **2005**, *1*, 953–962.
[66] R. E. Stratmann, G. E. Scuseria, M. J. Frisch, *J. Chem. Phys.* **1998**, *109*, 8218.
[67] R. Dennington, T. Keith, J. Millam, *Gaussview*, version 5, Semichem Inc., Shawnee Mission, KS, **2009**.
[68] N. M. O'Boyle, A. L. Tenderholt, K. M. Langner, *J. Comput. Chem.* **2008**, *29*, 839–845.

Received: April 23, 2017